Journal of Inclusion Phenomena and Molecular Recognition in Chemistry **16:** 25–54, 1993.

Studies on Werner Clathrates. Part 13.[1] Selective Criteria in Werner Clathrates. Six Crystal Structures with Bis(isothiocyanato)tetra(4-vinylpyridine)nickel(II) as Host

LAURENCE LAVELLE* ** and LUIGI R. NASSIMBENI
Department of Physical Chemistry, University of Cape Town, Rondebosch 7700, South Africa.

(Received: 22 February 1993; in final form: 20 August 1993)

Abstract. This paper addresses the general question: what are the significant guest properties selected by this host when interacting with guest molecules in the liquid phase, resulting in cocrystallization of the host and guest? In particular, to what extent do π electrons in a guest molecule effect its potential as a guest? Werner clathrates of the host $[Ni(NCS)_2(4\text{-}ViPy)_4]$ with mixtures of tetrahydrofuran (THF) and cyclic hydrocarbons as guests have been synthesised and their structures elucidated. Clathrate (**1**): $[Ni(NCS)_2(4\text{-}ViPy)_4](1.78$ THF$)(0.22$ cyclohexane), crystallizes in the orthorhombic space group P_{bcn} $a = 9.976(6)$, $b = 20.630(25)$, $c = 19.861(4)$Å, $V = 4087$Å^3, $Z = 4$, $R = 0.087$ for 1461 reflections; (**2**): $[Ni(NCS)_2(4\text{-}ViPy)_4](1.76$ THF$)(0.24$ cyclohexene), P_{bcn}, $a = 9.987(7)$, $b = 20.614(4)$, $c = 19.898(4)$Å, $V = 4096$Å^3, $Z = 4$, $R = 0.084$ for 1304 reflections; (**3**): $[Ni(NCS)_2(4\text{-}ViPy)_4](0.48$ THF$)(0.52$ 1,3-cyclohexadiene), tetragonal $I4_1/a$, $a = 16.898(3)$, $b = 16.898(3)$, $c = 26.463(6)$Å, $V = 7556$Å^3, $Z = 8$, $R = 0.120$ for 1698 reflections; (**4**): $[Ni(NCS)_2(4\text{-}ViPy)_4](0.36$ THF$)(1.04$ 1,4-cyclohexadiene), $I4_1/a$, $a = 16.986(4)$, $b = 16.986(4)$, $c = 25.896(15)$Å, $V = 7472$Å^3, $Z = 8$, $R = 0.103$ for 2025 reflections; (**5**): $[Ni(NCS)_2(4\text{-}ViPy)_4](0.35$ THF$)(1.05$ benzene), $I4_1/a$, $a = 17.102(10)$, $b = 17.102(10)$, $c = 25.498(8)$Å, $V = 7458$Å^3, $Z = 8$, $R = 0.118$ for 2200 reflections; (**6**): $[Ni(NCS)_2(4\text{-}ViPy)_4](3$ benzene), triclinic $P\bar{1}$, $a = 10.432(24)$, $b = 11.155(9)$, $c = 21.581(7)$Å, $\alpha = 78.70(5)$, $\beta = 82.60(7)$, $\gamma = 74.09(13)^\circ$, $V = 2361$Å^3, $Z = 2$, $R = 0.078$ for 3427 reflections. Host–guest ratios and, for mixtures of guests, guest1/guest2 ratios, were elucidated by density and NMR. We show that the conformational freedom of the substituted pyridines is not the primary reason for the clathrating ability of Werner hosts. All six structures show no host–guest interaction at the level of van der Waals interactions. As non-bonding interactions are not observed between the host and guest, this study shows that the above host's selectivity by enclathration of particular guest molecules cannot be accounted for by solid state structural analysis.

Key words: Werner clathrate, nickel octahedral complex, tetrahydrofuran, crystal structure, NMR, molecular recognition, hydrocarbon.

Supplementary Data relating to this article are deposited with the British Library as Supplementary Publication No. SUP 82153 (84 pages).

* Author for correspondence
** Current Address: Department of Chemistry, Princeton University, Princeton, New Jersey 08544, U.S.A.

1. Introduction

Werner clathrates are complexes of the type MX_2L_4 where, M is a divalent transition metal cation, e.g. Ni^{2+}; X is an anionic ligand, e.g. NCS^-, NO_2^-, NCO^-, halide and L is an electrically neutral substituted pyridine, 1-arylalkylamine or isoquinoline. Interest in the enclathrating ability of these hosts was stimulated by Schaeffer and coworkers, who announced a new method of separating aromatics from petroleum fractions in 1957 [2]. Since then the host [$Ni(NCS)_2$(4-methylpyridine)$_4$] has received the most attention. Its enclathrating ability ranges from noble gases to condensed aromatics, in cavities of layer, channel or cage shape. The chromatographic abilities [3] of this host and the thermodynamics of enclathration [4] have been studied. The physicochemical behavior of the clathrates it forms with different guests has been reviewed by Lipkowski [5].

We have studied the clathrating ability of [$Ni(NCS)_2$(4-R-pyridine)$_4$] by varying the substituent, R on the base: R = H [29], ethyl [6], vinyl [7,8,9,28,29], *t*-butyl [1], phenyl [1,10,11,12,13], benzyl [1]. These studies have shown this type of host to cocrystallize with a variety of *neutral guest molecules* (*ortho*-bromoiodobenzene, *ortho*-, *meta*-, *para*-xylene, *para*-cymene, methyl cellosolve, dimethylsulphoxide, carbon disulphide, chloroform, carbon tetrachloride, diethylether) with the host–host and host–guest interaction almost always occurring via non-specific van der Waals interactions (dispersion forces).

The current rationale [5,13,34,35] of these observed host–guest interactions, resulting in cocrystallization with a particular guest, is that the guest has a suitable size and shape to fit in the void sites as a result of the host–host interaction, and the resulting favorable enthalpic contribution between the host and guest is from nonspecific (non-directional) van der Waals interactions for nonpolar guests and/or electrostatic interactions for polar guests. In this study we investigate a series of clathrates where, with a given host, the guest entity was changed systematically with the intention of characterizing the observed host–guest interactions in the crystal structure with a singly changing guest parameter. We thus chose a series of neutral cyclic hydrocarbons as guests, each having a skeleton of six carbon atoms, but where the number of double bonds varied from zero to three: cyclohexane, cyclohexene, 1,3-cyclohexadiene, 1,4-cyclohexadiene and benzene.

We now report the crystal structures of the clathrates:

[$Ni(NCS)_2$(4-ViPy)$_4$](1.78 THF)(0.22 cyclohexane)	**(1)**
[$Ni(NCS)_2$(4-ViPy)$_4$](1.76 THF)(0.24 cyclohexene)	**(2)**
[$Ni(NCS)_2$(4-ViPy)$_4$](0.48 THF)(0.52 1,3-cyclohexadiene)	**(3)**
[$Ni(NCS)_2$(4-ViPy)$_4$](0.36 THF)(1.04 1,4-cyclohexadiene)	**(4)**
[$Ni(NCS)_2$(4-ViPy)$_4$](0.35 THF)(1.05 benzene)	**(5)**
[$Ni(NCS)_2$(4-ViPy)$_4$](3 benzene)	**(6)**
[$Ni(NCS)_2$(4-ViPy)$_4$](2 THF)	**(7)**

2. Experimental

2.1. PREPARATION OF HOST

All procedures, i.e.: bench work; crystal formation; visual observation; photography and mounting of crystals were carried out at room temperature, 293–303 K.

The host powder complex was prepared by dissolving $NiCl_2 \cdot 6H_2O$ (2.00 g, 8.4 mmol) and KNCS (1.64 g, 16.8 mmol) in glass-distilled water (20 mL), giving a green transparent solution of $Ni(NCS)_2$. Vinylpyridine (36.9 mmol, 10% excess) was added dropwise to the green solution with constant stirring. An immediate, fine, pale blue precipitate formed (host powder complex) which was stirred for an additional 30 min to ensure complete reaction. The precipitate was filtered, washed with distilled water (3×10 mL), air dried for 30 min and stored in a desiccator.

2.2. CRYSTAL GROWTH

As the host is not sufficiently soluble in cyclohexane, cyclohexene, 1,3-cyclohexadiene and 1,4-cyclohexadiene to obtain cystals, a stock solution of [Ni(NCS)$_2$(4-ViPy)$_4$] was prepared by dissolving 10.70 g of the complex in 50 mL of tetrahyrofuran giving a saturated solution of 29.0×10^{-3} mole fraction complex.

Previous studies had shown that THF is *not* included when used as a solvent with other guests (*ortho*-, *meta*-, *para*-xylene, chloroform [7] and *ortho*-bromoiodobenzene [28]). The procedure used here was as described in References 7 and 28.

Clathrates (**1**)–(**5**) were obtained by the method of layering or liquid diffusion [14]: 2.5 mL of the stock solution was layered with equal volumes of cyclohexane, cyclohexene, 1,3-cyclohexadiene, 1,4-cyclohexadiene and benzene, respectively, and the vials sealed. Crystals of clathrates (**1**) and (**2**) were observed at the layered solvent interface after 15 min. Clathrate (3) formed after 3 days at the bottom of the vial. Clathrates (**4**) and (**5**) formed at the bottom of the vials only after they were unsealed to allow evaporation: crystals formed after 12 days. Clathrates (**6**) and (**7**) were obtained from saturated solutions of benzene and THF, respectively, after solvent evaporation for 3–5 days. All crystals were dark blue.

2.3. ^{1}H NMR SPECTRA

Spectra were recorded on a Bruker WH-90 spectrometer, (90.02 MHz); using $CDCl_3$ as solvent and $SiMe_4$ as standard. For clathrates (**1**)–(**5**) a *single large crystal* was removed from its mother liquor, 'washed' with 2 or 3 drops of $CDCl_3$ and then dissolved in $CDCl_3$. See Table I.

TABLE I. NMR data of guest molecules for clathrates (**1**)–(**5**).

Compound	δ	Integration
(**1**)	1.40,12H, cyclohexane(1.42)*	cyclohexane : THF
	1.96,4H, THF(1.83)	1 : 8
(**2**)	5.64,2H, cyclohexene(5.69)	cyclohexene : THF
	3.64,4H, THF(3.70)	1 : 7
(**3**)	5.82,4H, 1,3-cyclohexadiene(5.80)	1,3-cyclohexadiene : THF
	3.70,4H, THF(3.70)	1.1 : 1
(**4**)	5.68,4H, 1,4-cyclohexadiene(5.68)	1,4-cyclohexadiene : THF
	1.92,4H, THF(1.83)	2.9 : 1
(**5**)	7.36,6H, benzene(7.40)	benzene : THF
	1.88,4H, THF(1.83)	3 : 1

* The corresponding chemical shift value for the pure compound [30] is given in brackets.

2.4. CRYSTALLOGRAPHY

To avoid deterioration through guest desorption, all crystals were kept in contact with their mother liquor at all times. Single crystals were cut to a suitable size and mounted firmly in Lindemann tubes together with mother liquor. Density measurements were carried out by flotation in mixtures of cyclohexane, CCl_4 and 1,2-dichlorobenzene, measuring the density of the solution with an Anton Paar DMA 35 density meter. For crystals (**1**)–(**5**), once the ratios of the guests were known from their NMR spectra, the *correct* host : total guest ratio could be calculated using the measured densities of the crystals. The following equation was used:

$$Z_H(M_H) + Z_G[N_{G1}(M_{G1}) + N_{G2}(M_{G2})] = ND_m \text{ Vol} \times 10^{-24}$$

where

Z_H = number of host molecules per unit cell;
Z_G = number of guest molecules per unit cell;
N_{G1} = ratio of guest type one;
N_{G2} = ratio of guest type two;
M_H = molecular weight of host in g mol^{-1};
M_{G1} = molecular weight of guest type one in g mol^{-1};
M_{G2} = molecular weight of guest type two in g mol^{-1};
N = Avogadro constant (6.023×10^{23});
D_m = measured density in g cm^{-3};
Vol = Volume of unit cell in Å^3.

For example, for structure (**1**): $Z_H = 4$, $M_H = 595.42$, $M_{G1} = 72.12$, $M_{G2} = 84.16$, $D_m = 1.21$, Vol = 4087.49 giving $Z_G = 8$.

TABLE II. Crystal data for clathrates (**1**)–(**7**).

Compound	(**1**)	(**2**)	(**3**)	(**4**)
Guest 1	THF	THF	THF	THF
Guest 2	cyclohexane	cyclohexene	1,3-cyclo-hexadiene	1,4-cyclo-hexadiene
H:G1:G2	1:1.78:0.22	1:1.76:0.24	1:0.48:0.52	1:0.36:1.04
M/g mol^{-1}	742.31	742.07	671.71	704.70
D_m/g cm^{-3}	1.21	1.20	1.18	1.25
μ(Mo-K_α)/ cm^{-1}	5.67	5.66	6.08	6.17
F(000)	1566.99	1564.75	2816.54	3045.82
Space group	P_{bcn}	P_{bcn}	$I4_1/a$	$I4_1/a$
a/Å	9.976(6)	9.987(7)	16.898(3)	16.986(4)
b/Å	20.630(25)	20.614(4)	16.898(3)	16.986(4)
c/Å	19.861(4)	19.898(4)	26.463(6)	25.896(15)
V/Å^3	4087.49	4096.44	7556.31	7471.62
Z	4	4	8	8
Compound	(**5**)	(**6**)	(**7**)	
Guest 1	THF	benzene	THF	
Guest 2	benzene	–	–	
H:G1:G2	1:0.35:1.05	1:3	1:2	
M/g mol^{-1}	702.69	860.02	739.71	
D_m/g cm^{-3}	1.25	1.17	1.21	
μ(Mo-K_α)/ cm^{-1}	6.17	4.92	6.17	
F(000)	2944.70	872.0	1560	
Space group	$I4_1/a$	$P\bar{1}$	P_{bcn}	
a/Å	17.102(10)	10.432(24)	9.937(4)	
b/Å	17.102(10)	11.155(9)	20.634(4)	
c/Å	25.498(8)	21.581(7)	19.842(8)	
α/°	–	78.70(5)	–	
β/°	–	82.60(7)	–	
γ/°	–	74.09(13)	–	
V/Å^3	7457.61	2360.82	4068.40	
Z	8	2	4	

H = HOST; G1 = GUEST 1; G2 = GUEST 2

The host : total guest ratios thus obtained were confirmed by thermo-gravimetric analysis, which yielded similar results [31].

Crystal data for clathrates (**1**)–(**7**) are listed in Table II.

2.5. DATA COLLECTION AND PROCESSING

Cell parameters were determined by least-squares analysis of 24 reflections measured in the range 16 to 17° in θ automatically located and centered on an Enraf-Nonius CAD4 diffractometer with graphite monochromated MoK_α radiation ($\lambda = 0.7107$ Å). Intensity data were collected at 294 K in the $\omega - 2\theta$ scan mode with a final acceptance limit of 20σ at 20° min^{-1} in ω and a maximum recording time of 40 s. The vertical aperture width was fixed at 6 mm and for each structure: *(i)* the aperture width was set according to $(x + 1.05 \tan \theta)$mm; *(ii)* the scan width, in ω, was set according to $(y + 0.35 \tan \theta)°$.

Table III lists values of scan and aperture widths for each structure. The intensity of three reference reflections was monitored every hour to ascertain both instrumental stability and crystal decomposition. Recentering was carried out every 100 measured reflections. All intensities were corrected for Lorentz and polarisation factors and an empirical absorption correction [15] was applied to each data set. For clathrates (**1**) and (**2**) there was crystal decay which was compensated by a decay correction. Experimental and refinement parameters for clathrates (**1**)–(**6**) are listed in Table III.

Clathrate (**7**) has the same cell parameters as clathrates (**1**) and (**2**). A trial data collection in the range 1–10° in θ showed that the intensities matched those of (**1**) and (**2**), and (**7**) was therefore deemed isomorphous with them.

2.6. STRUCTURE SOLUTION

All structures (**1**)–(**6**) were solved using the heavy-atom method, subsequent difference Fourier syntheses and refinement by full-matrix least squares with the SHELX 76 program system [16]. For structures (**1**)–(**5**) location of the guest molecules required the contouring of electron density maps. The program SHELX 400 was used for structure (**6**) owing to the large number of parameters. Hydrogen atoms were geometrically positioned with respect to their parent carbons and allowed to ride on the carbon atoms to which they were bonded. The C–H bond distances were fixed at 1.00 Å with the temperature factors of hydrogens linked. No hydrogens were included for the guest molecules. When atoms on special positions were treated anisotropically, symmetry restrictions were applied according to Peterse and Palm [17]. Atomic radii were those of Pauling [18]. Scattering factors for all nonhydrogen atoms were from Cromer and Mann [19] and those for the hydrogen atoms from Stewart *et al.* [20]. The final model employed anisotropic thermal parameters for the heavy atoms, Ni and S. The program PLUTO [24] was used to draw individual molecules and to study their molecular packing. PARST [25] was used for all molecular geometry calculations, torsion angles and *intermolecular contacts*. The program ALCHEMY [26] was used to calculate the coordinates of the model cyclohexane and cyclohexene, which were used in the program MULTAN [27]. The MULTAN 78 program NORMAL was used to calculate the spherically aver-

TABLE III. Experimental and refinement parameters for clathrates (**1**)–(**6**).

Compound	(**1**)	(**2**)	(**3**)
Crystal dimensions/mm	0.25 × 0.5 × 0.74	0.42 × 0.5 × 0.55	0.5 × 0.5 × 0.56
Scan width	1.00	1.05	1.00
Aperture width	1.50	1.20	1.20
Total number of reflections	2606	2497	2628
Total number observed[a]	1461	1304	1698
Crystal stability/%	17.2	32.4	8.7
Average decay correction factor	1.04634	1.09387	–
No. of variables	97	97	88
R^b	0.087	0.084	0.120
R^c	0.100	0.096	0.125
Weighting scheme w	$(\sigma^2F + 0.0020F^2)^{-1}$	$(\sigma^2F + 0.0020F^2)^{-1}$	$(\sigma^2F + 0.0226F^2)^{-1}$
Compound	(**4**)	(**5**)	(**6**)
Crystal dimensions/mm	0.47 × 0.5 × 0.53	0.5 × 0.5 × 0.56	0.53 × 0.56 × 0.56
Scan width	1.00	0.85	0.95
Aperture width	1.40	1.15	1.20
Total number of reflections	3002	2823	3985
Total number observed[a]	2025	2200	3427
Crystal stability/%	3.2	5.9	6.9
No. of variables	88	88	293
R^b	0.103	0.118	0.078
R^c	0.112	0.132	0.085
Weighting scheme w	$(\sigma^2F + 0.0046F^2)^{-1}$	$(\sigma^2F + 0.0203F^2)^{-1}$	$(\sigma^2F + 0.0001F^2)^{-1}$

[a] $I_{rel} > 2\sigma I_{rel}$; [b] $R = \Sigma||F_0| - |F_c||/\Sigma|F_0|$; [c] $R = \Sigma w^{1/2}\,||F_0| - |F_c||/\Sigma w^{1/2}\,|F_0|$.

aged molecular scattering factor for cyclohexane and cyclohexene, in structures (**1**) and (**2**), respectively.

OPEC [33] was used to map precisely the sizes and shapes of the guest cavities and to confirm the poor packing of the structures. The method underlying this packing analysis is that each atom in the structure is assigned a rigid sphere of radius $R_{m,i}$ (van der Waals radii). This sphere may interpenetrate, with spheres

associated to other atoms on the same molecule, bound or not bound to atom i and with spheres associated with atoms on neighbouring molecules. Each point in the cell space, as described by a vector s, can be either inside one or more of the atomic spheres or outside. The element of volume, dv, centered at s is accordingly labelled as either occupied (by a finite number representing the packing density) or unoccupied (by 0). In all the diagrams obtained from OPEC the 0s have been deleted to facilitate observation of the unoccupied cavities and each cross-section is a representation of the unit cell, i.e. drawn to scale.

Structures (**1**) and (**2**) are isomorphous with respect to the host only. In the space group P_{bcn} the nickel atom and two vinylpyridine ligands are located on the diad at Wyckoff position c.

From the NMR spectrum it was known that both THF and cyclohexane were present in the ratio 0.89 : 0.11 in (**1**). Modelling of residual electron density with THF at Wyckoff general position d with site occupancy 0.89 was acceptable for structure (**1**).

For structure (**2**) the same procedure was followed with the THF atoms having site occupancy 0.88. In order to take the electron density of cyclohexane and cyclohexene into account, a spherically averaged molecular scattering factor was calculated for cyclohexane and cyclohexene. These spherically averaged groups were placed at the centre of the THF guest molecule with a site occupancy of 0.11 and 0.12 respectively and refined isotropically. This model of incorporating cyclohexane and cyclohexene was not successful and was discarded. Thus in structures (**1**) and (**2**) the only guest which was modeled was THF. The final fractional atomic coordinates are given in Table IV.

On the basis of unit cell parameters, reflection conditions and intensities, crystal density and thermogravimetric analysis [31] structure (**7**) is isomorphous with structures (**1**) and (**2**).

Structures (**3**), (**4**) and (**5**) are isomorphous with respect to the host only. All of these $I4_1/a$ structures are reported with respect to the second origin choice at $\bar{1}$. The nickel atom is at Wyckoff special position e, and is the only host atom to lie on the diad.

For structure (**3**) the presence of guest (electron density of several e/Å^3) was located around the centre of inversion, Wyckoff position d. In agreement with the density and NMR data, 1,3-cyclohexadiene (regular hexagon, average bond length = 1.47 Å, site occupancy = 0.26) and THF (regular pentagon, average bond length = 1.49 Å, site occupancy = 0.24) were used as a fit to the difference electron density map in this region. After several other models were attempted, this approximation of the guest modelling was acceptable with the average temperature factor of the guest atoms being 0.34 Å^2, a high but acceptable value for disordered guests of these compounds. The final fractional atomic coordinates are given in Table V.

For structure (**4**) the same results were obtained but with a more diffuse electron density about the inversion centre extending to the $\bar{4}$ site. The same procedure as

TABLE IV. Fractional atomic coordinates ($\times 10^4$) with e.s.d.s in parenthesis for compounds (**1**) and (**2**).

Compound (**1**) Atom	x	y	z	Compound (**2**) Atom	x	y	z
Ni(1)	0	1839(1)	2500(0)	Ni(1)	0	1842(1)	2500(0)
N(1)	–1851(8)	1846(4)	2020(4)	N(1)	–1838(9)	1844(4)	2029(4)
C(1)	–2851(11)	1864(5)	1773(6)	C(1)	–2866(11)	1862(5)	1785(6)
S(1)	–4292(4)	1888(3)	1404(2)	S(1)	–4283(4)	1884(3)	1404(3)
N(11)	0(0)	804(6)	2500(0)	N(11)	0(0)	791(6)	2500(0)
C(12)	–540(11)	462(6)	2002(6)	C(12)	–550(11)	463(6)	2010(6)
C(13)	–514(12)	–216(6)	2000(6)	C(13)	–554(12)	–202(6)	2009(6)
C(14)	0(0)	–564(9)	2500(0)	C(14)	0(0)	–558(10)	2500(0)
C(17)	0(0)	–1202(15)	2500(0)	C(17)	0(0)	–1300(17)	2500(0)
C(18)	–201(35)	–1718(17)	2145(20)	C(18)	–219(40)	–1578(22)	2062(25)
N(21)	0(0)	2873(6)	2500(0)	N(21)	0(0)	2875(6)	2500(0)
C(22)	1114(11)	3205(5)	2361(5)	C(22)	1101(12)	3207(5)	2355(5)
C(23)	1113(12)	3887(6)	2368(5)	C(23)	1106(13)	3880(6)	2358(6)
C(24)	0(0)	4219(9)	2500(0)	C(24)	0(0)	4219(10)	2500(0)
C(27)	0(0)	4924(15)	2500(0)	C(27)	0(0)	4924(19)	2500(0)
C(28)	–635(46)	5329(21)	2401(25)	C(28)	–635(63)	5328(28)	2490(30)
N(41)	–960(7)	1839(4)	3462(4)	N(41)	–941(8)	1823(4)	3460(4)
C(42)	–2046(11)	1500(5)	3557(6)	C(42)	–2041(11)	1491(5)	3570(6)
C(43)	–2622(11)	1428(6)	4224(6)	C(43)	–2597(12)	1414(6)	4206(6)
C(44)	–2024(11)	1761(5)	4732(6)	C(44)	–2039(12)	1742(6)	4736(6)
C(45)	–964(12)	2124(6)	4615(6)	C(45)	–919(12)	2113(6)	4624(6)
C(46)	–411(11)	2169(5)	3982(6)	C(46)	–411(11)	2151(6)	3982(6)
C(47)	–2525(17)	1680(9)	5447(9)	C(47)	–2569(18)	1693(8)	5471(8)
C(48)	–3482(19)	1304(9)	5661(9)	C(48)	–3486(21)	1297(9)	5635(10)
C(1G)	2837(0)	4710(0)	–282(0)	C(1G)	2659(0)	4657(0)	–206(0)
C(2G)	3788(0)	4290(0)	104(0)	C(2G)	2080(0)	4677(0)	507(0)
C(3G)	3416(0)	3852(0)	672(0)	C(3G)	2980(0)	4288(0)	979(0)
C(4G)	1940(0)	3918(0)	625(0)	C(4G)	3299(0)	3799(0)	499(0)
C(5G)	1804(0)	5432(0)	228(0)	C(5G)	3834(0)	4226(0)	2(0)

for structure (**3**) was followed but with the six atoms of 1,4-cyclohexadiene having site occupancy 0.52 and the five atoms of THF having site occupancy 0.18. The final fractional atomic coordinates are given in Table V.

For structure (**5**) the same procedure was followed as for structure (**4**) but with the average bond length of benzene = 1.40 Å, site occupancy = 0.53 and the site occupancy of the THF atoms = 0.17. The final fractional atomic coordinates are given in Table VI.

For structure (**6**) the nickel atom is at Wyckoff general position i in the space group $P\bar{1}$. In confirmation with the density three benzene rings were located. As

TABLE V. Fractional atomic coordinates ($\times 10^4$) with e.s.d.s in parenthesis for compounds (**3**) and (**4**).

Compound (**3**) Atom	x	y	z	Compound (**4**) Atom	x	y	z
Ni(1)	5000(0)	2500(0)	5441(1)	Ni(1)	5000(0)	2500(0)	5477(1)
N(1)	4017(5)	3242(5)	5428(3)	N(1)	4010(4)	3234(4)	5464(2)
C(1)	3363(7)	3421(7)	5425(4)	C(1)	3372(5)	3403(5)	5480(3)
S(1)	2443(2)	3660(3)	5411(2)	S(1)	2463(2)	3687(2)	5508(2)
N(11)	5502(5)	3218(5)	6020(3)	N(11)	5486(4)	3216(4)	6068(3)
C(12)	5033(7)	3515(7)	6387(4)	C(12)	5020(6)	3520(5)	6435(4)
C(13)	5332(7)	3946(7)	6781(5)	C(13)	5324(6)	3964(6)	6853(4)
C(14)	6173(7)	4050(7)	6820(5)	C(14)	6155(6)	4081(5)	6889(3)
C(15)	6600(7)	3735(7)	6458(5)	C(15)	6609(6)	3775(5)	6517(4)
C(16)	6278(7)	3346(7)	6070(4)	C(16)	6256(5)	3339(5)	6118(3)
C(17)	6543(8)	4433(8)	7260(5)	C(17)	6533(7)	4488(6)	7309(5)
C(18)	6215(10)	4629(11)	7672(7)	C(18)	6182(10)	4675(11)	7747(7)
N(21)	4448(5)	1802(5)	4868(3)	N(21)	4442(4)	1820(3)	4890(2)
C(22)	4063(6)	2169(7)	4477(4)	C(22)	4079(5)	2162(5)	4486(3)
C(23)	3735(7)	1767(7)	4081(4)	C(23)	3733(5)	1771(5)	4087(3)
C(24)	3759(6)	936(6)	4074(4)	C(24)	3751(5)	954(5)	4083(3)
C(25)	4144(7)	573(7)	4468(4)	C(25)	4129(5)	592(5)	4490(3)
C(26)	4466(6)	1030(6)	4858(4)	C(26)	4457(5)	1014(5)	4880(3)
C(27)	3423(9)	493(10)	3654(6)	C(27)	3442(7)	490(7)	3658(4)
C(28)	3126(14)	675(14)	3275(9)	C(28)	3145(9)	774(9)	3223(6)
C(1G)	2673(0)	2223(0)	7320(0)	C(1G)	1310(0)	3262(0)	7108(0)
C(2G)	3473(0)	1981(0)	7472(0)	C(2G)	0710(0)	3230(0)	6699(0)
C(3G)	3780(0)	2200(0)	7972(0)	C(3G)	0591(0)	2498(0)	6406(0)
C(4G)	3285(0)	2663(0)	8321(0)	C(4G)	1070(0)	1800(0)	6521(0)
C(5G)	2484(0)	2905(0)	8169(0)	C(5G)	1669(0)	1833(0)	6930(0)
C(6G)	2178(0)	2686(0)	7669(0)	C(6G)	1789(0)	2564(0)	7224(0)
C(11G)	2403(0)	2368(0)	7362(0)	C(11G)	2260(0)	3086(0)	7321(0)
C(22G)	3220(0)	2044(0)	7408(0)	C(22G)	2811(0)	3102(0)	7769(0)
C(33G)	3533(0)	2271(0)	7914(0)	C(33G)	3023(0)	2274(0)	7898(0)
C(44G)	2910(0)	2736(0)	8180(0)	C(44G)	2605(0)	1746(0)	7529(0)
C(55G)	2212(0)	2796(0)	7839(0)	C(55G)	2133(0)	2248(0)	7173(0)

shown in Figure 1 two benzene rings at general positions are superimposed on each other with site occupancy 0.5 (static disorder). The second and third benzene molecules were located with three peaks around the $\bar{1}$ sites, Wyckoff position d and Wyckoff position a, and were given full site occupancy. The bond lengths, angles and temperature factors for each of the three peaks gave no indication of disorder around the centre of symmetry. This was the only structure where we were able to refine the guest atoms without any approximate models.

TABLE VI. Fractional atomic coordinates ($\times 10^4$) with e.s.d.s in parenthesis for compounds (**5**) and (**6**).

Compound (**5**)				Compound (**6**) *continued*			
Atom	x	y	z	Atom	x	y	z
Ni(1)	5000(0)	2500(0)	5527(0)	C(16)	520(8)	3801(8)	3500(4)
N(1)	4012(4)	3216(4)	5511(2)	C(17)	1141(10)	6392(9)	4189(4)
C(1)	3385(5)	3416(5)	5521(3)	C(18)	2017(11)	6847(10)	4376(5)
S(1)	2479(2)	3711(2)	5542(1)	N(21)	782(6)	2754(6)	2117(3)
N(11)	5486(4)	3209(4)	6128(2)	C(22)	–285(9)	2426(8)	1985(4)
C(12)	5025(6)	3531(6)	6489(4)	C(23)	–1112(10)	3165(9)	1513(5)
C(13)	5323(6)	3988(6)	6903(4)	C(24)	–828(10)	4250(10)	1166(5)
C(14)	6140(6)	4090(6)	6943(3)	C(25)	237(10)	4582(9)	1305(5)
C(15)	6585(6)	3781(6)	6574(3)	C(26)	1025(9)	3845(9)	1777(4)
C(16)	6260(5)	3341(5)	6169(3)	C(27)	–1621(14)	5139(14)	647(6)
C(17)	6532(8)	4534(8)	7366(5)	C(28)	–2567(19)	4921(20)	447(10)
C(18)	6154(13)	4648(13)	7793(9)	N(31)	2396(6)	0(5)	2372(3)
N(21)	4446(3)	1823(3)	4919(2)	C(32)	2672(8)	33(8)	1762(4)
C(22)	4079(5)	2169(5)	4523(3)	C(33)	3057(8)	–981(8)	1453(4)
C(23)	3744(4)	1779(5)	4111(3)	C(34)	2983(8)	–2183(8)	1826(4)
C(24)	3755(5)	987(5)	4101(3)	C(35)	2617(8)	–2201(8)	2445(4)
C(25)	4127(5)	600(5)	4523(3)	C(36)	2321(8)	–1134(7)	2710(4)
C(26)	4459(4)	1029(4)	4910(3)	C(37)	3297(10)	–3348(10)	1530(5)
C(27)	3445(7)	531(7)	3671(4)	C(38)	3526(14)	–3418(13)	921(7)
C(28)	3130(9)	816(10)	3211(6)	N(41)	3370(6)	460(5)	3522(3)
C(1G)	2172(0)	3099(0)	7208(0)	C(42)	4648(8)	–95(7)	3339(4)
C(2G)	1545(0)	3548(0)	7025(0)	C(43)	5525(8)	–909(7)	3753(4)
C(3G)	0893(0)	3181(0)	6802(0)	C(44)	5128(7)	–1200(7)	4378(3)
C(4G)	0869(0)	2365(0)	6761(0)	C(45)	3808(7)	–616(7)	4569(4)
C(5G)	1497(0)	1916(0)	6944(0)	C(46)	2996(8)	180(7)	4129(4)
C(6G)	2149(0)	2283(0)	7167(0)	C(47)	6000(8)	–2079(8)	4844(4)
C(11G)	2038(0)	2832(0)	7193(0)	C(48)	7290(10)	–2699(9)	4715(5)
C(22G)	2264(0)	3408(0)	7604(0)	C(1G1)	2321(35)	150(31)	7743(17)
C(33G)	2830(0)	3023(0)	7965(0)	C(2G1)	1094(36)	1232(49)	7479(18)
C(44G)	2955(0)	2207(0)	7777(0)	C(3G1)	948(27)	2492(31)	7595(14)
C(55G)	2466(0)	2089(0)	7300(0)	C(4G1)	1872(40)	2895(33)	7927(19)
				C(5G1)	2993(28)	1896(38)	8194(13)
Compound (**6**)				C(6G1)	3093(23)	586(24)	8078(11)
				C(1G2)	4224(13)	9543(12)	9679(6)
Ni(1)	2063(1)	1597(1)	2826(0)	C(2G2)	5494(14)	8822(12)	9792(6)
N(1)	3660(6)	2117(6)	2261(3)	C(3G2)	6265(13)	9276(13)	135(6)
C(1)	4360(7)	2512(7)	1863(4)	C(1G3)	–3991(26)	5648(26)	3326(23)
S(1)	5292(3)	3082(3)	1313(1)	C(2G3)	–3579(33)	4816(41)	3905(19)
N(2)	452(6)	1090(6)	3352(3)	C(3G3)	–3255(33)	3574(37)	4028(18)
C(2)	–224(8)	578(7)	3698(4)	C(4G3)	–3306(21)	3060(20)	3460(18)
S(2)	–1179(3)	–158(3)	4177(2)	C(5G3)	–3757(33)	3887(43)	2859(19)
N(11)	1768(6)	3165(5)	3288(3)	C(6G3)	–3999(33)	5036(43)	2861(19)
C(12)	2763(8)	3599(7)	3394(4)	C(1G4)	293(14)	–305(17)	–580(7)
C(13)	2648(8)	4607(7)	3678(4)	C(2G4)	340(15)	8717(15)	–70(9)
C(14)	1369(8)	5278(8)	3894(4)	C(3G4)	34(14)	9067(15)	542(7)
C(15)	336(9)	4836(8)	3793(4)				

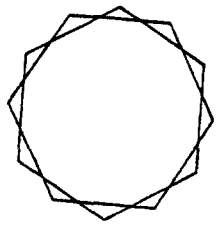

Fig. 1. Superimposed benzene rings.

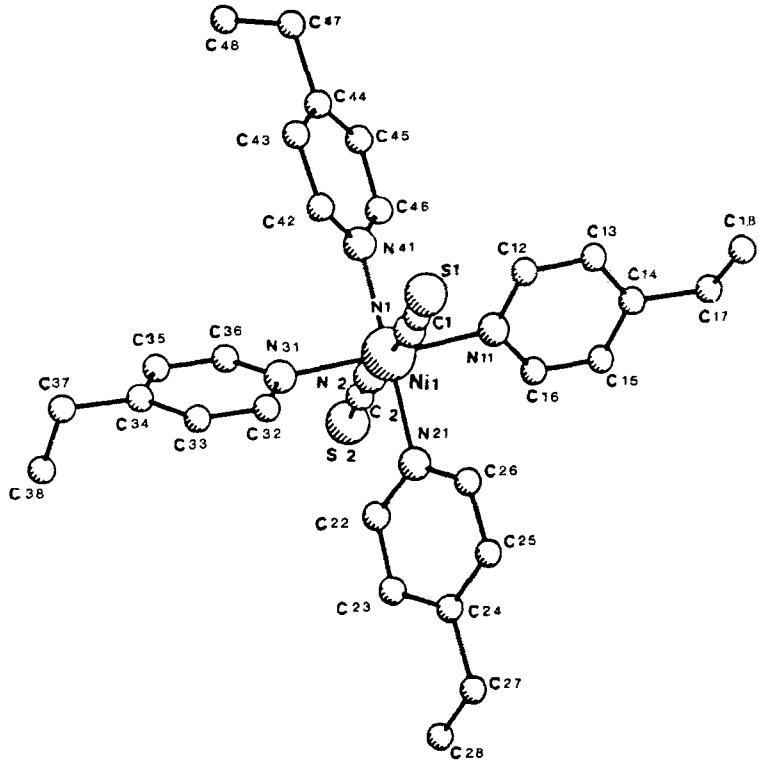

Fig. 2. Perspective view of host conformation with atomic nomenclature.

Attempted solution of the structure in space group $P1$ resulted in extensive correlation in the least-squares matrix and $R = 14\%$, thus substantiating the choice of the centrosymmetric space group $P\bar{1}$. The final fractional atomic coordinates are given in Table VI.

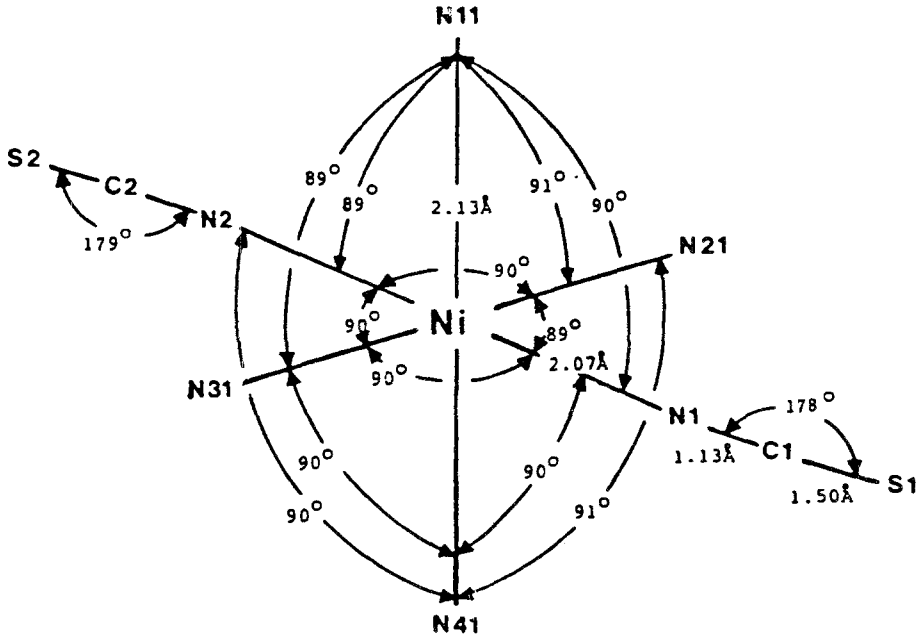

Fig. 3a. Typical environment of a nickel atom.

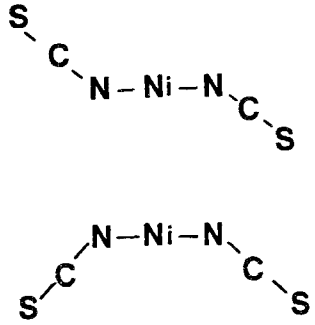

Fig. 3b. Different conformations of the isothiocyanate ligands as found in the clathrates (*trans*) and the clathrand (α-phase, *cis*).

3. Results and Discussion

3.1. General

The structure of the host in all the clathrates has the central nickel atom in an octahedral configuration with the isothiocyanate ligands in the *trans* position and the 4-vinylpyridine ligands in the propeller conformation (Figure 2). This propeller conformation is similar to those found in previous structures, irrespective of the

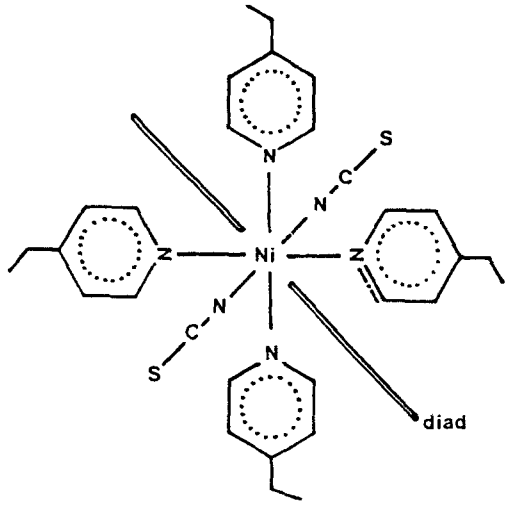

Fig. 4. Illustration of the ligands about the diad showing two 4-vinylpyridines and one isothiocyanate ligand as the asymmetric unit.

crystallographic phase [5]. An illustration of the typical environment of the nickel atom is shown in Figure 3a. As previously observed in complexes of this type [7,8,23] the Ni–N bond of the isothiocyanate ligands is shorter than the Ni–N bond of the pyridine ligands. In each structure the nickel atom is positioned in the molecular plane of the four pyridine nitrogen atoms. Angles subtended at the nickel atom vary from 86.8(2) to 92.4(3)° for the *cis* ligands and 176.3(3) to 180.0(4)° for the *trans* ligands. Previous work [28] has shown the isothiocyanate ligands to be linear, a symmetry condition imposed by sitting directly on the diad. In structures (**1**)–(**6**) the Ni–N_{cs}–C_s bond angles range from 158.0(7) to 166.4(8)° and the N_{cs}–C_s–S bond angles range from 177.0(1) to 179.4(8)°.

When the Ni–N_{cs}–C_s bond angle differs from 180°, the conformation of the NCS group around the Ni–N coordination bond plays an important role in determining the overall molecular shape of the host complex. In all the clathrate structures the isothiocyanate ligands are *trans* with respect to the sulphurs, irrespective of whether twofold or inversion symmetry of the host molecule has imposed this condition. For the α-phase [7] the isothiocyanate ligands are *cis* with respect to the sulphurs, as shown in Figure 3b.

3.2. CLATHRATES (**1**) AND (**2**)

The observed bond lengths and angles in structures (**1**)–(**6**) do not require special comment, with the exception of structures (**1**) and (**2**), which have the nickel at Wyckoff special position *c* and two of the 4-vinylpyridine ligands sitting along the diad. This results in distortion of the following bonds.

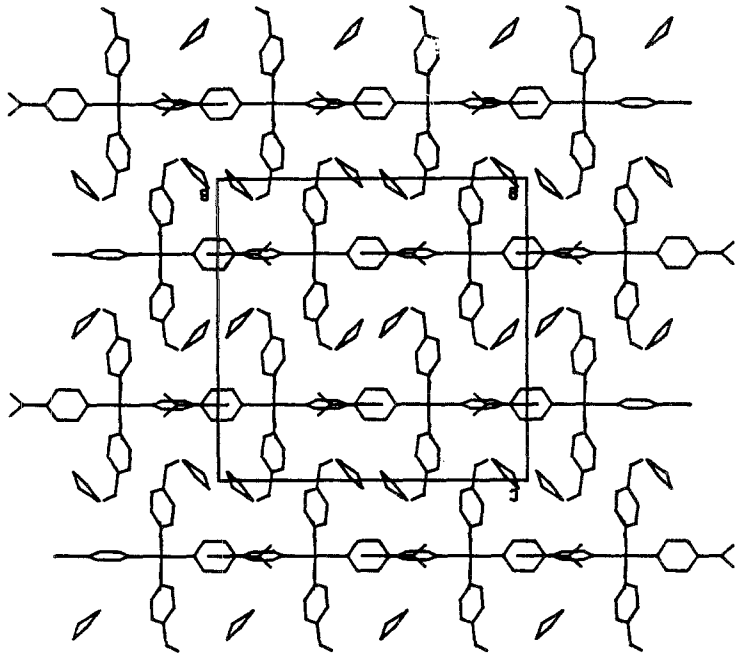

Fig. 5a. Molecular packing in structure (**1**) viewed down the x-axis.

(**1**): Ni–N_{py} along the diad, both are 2.06(1)Å (shortening);
Ni–N_{py} general position, 2.204(8)Å (lengthening);
N_{ring}–C_{ring} general position, 1.29(1)Å (shortening) and 1.37(1)Å (lengthening);
C_{ring}–C_{ring} general position, 1.30(2)Å (shortening) and 1.50(2)Å (lengthening);
C_{ring}–C_{vinyl} along the diad, 1.27(4)Å and 1.40(4)Å (shortening);
C_{vinyl}–C_{vinyl} disordered about the diad, 1.05(5)Å (shortening) and 1.29(3)Å (lengthening).

The isothiocyanate ligands are not significantly affected. The variations in structure (**2**) are similar but less extreme, only the Ni–N_{py} are shown:

(**2**): Ni–N_{py} along the diad, 2.09(1)Å and 2.06(1)Å;
Ni–N_{py} general position, 2.191(8)Å.

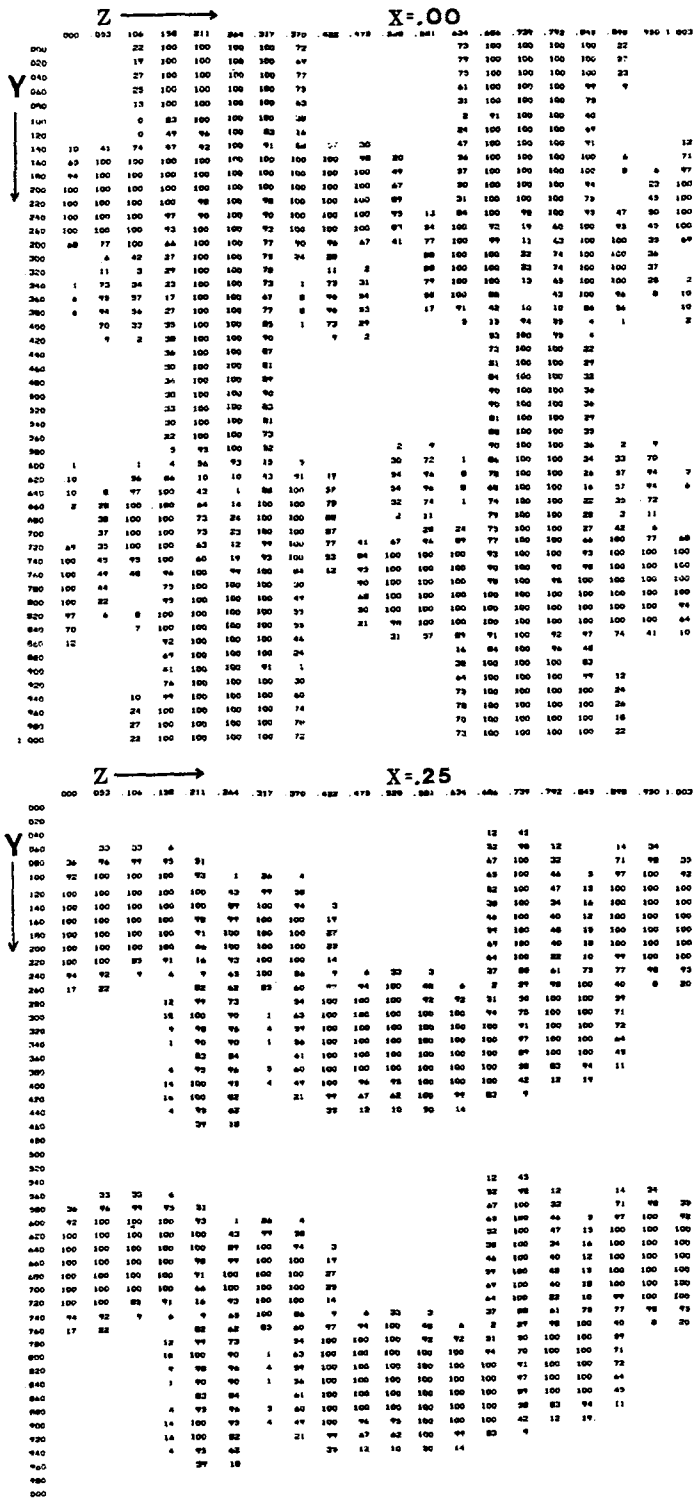

Fig. 5b. Packing diagrams of structure (**1**) with host only (hydrogens included) at $x = 0.0$ and $x = 0.25$.

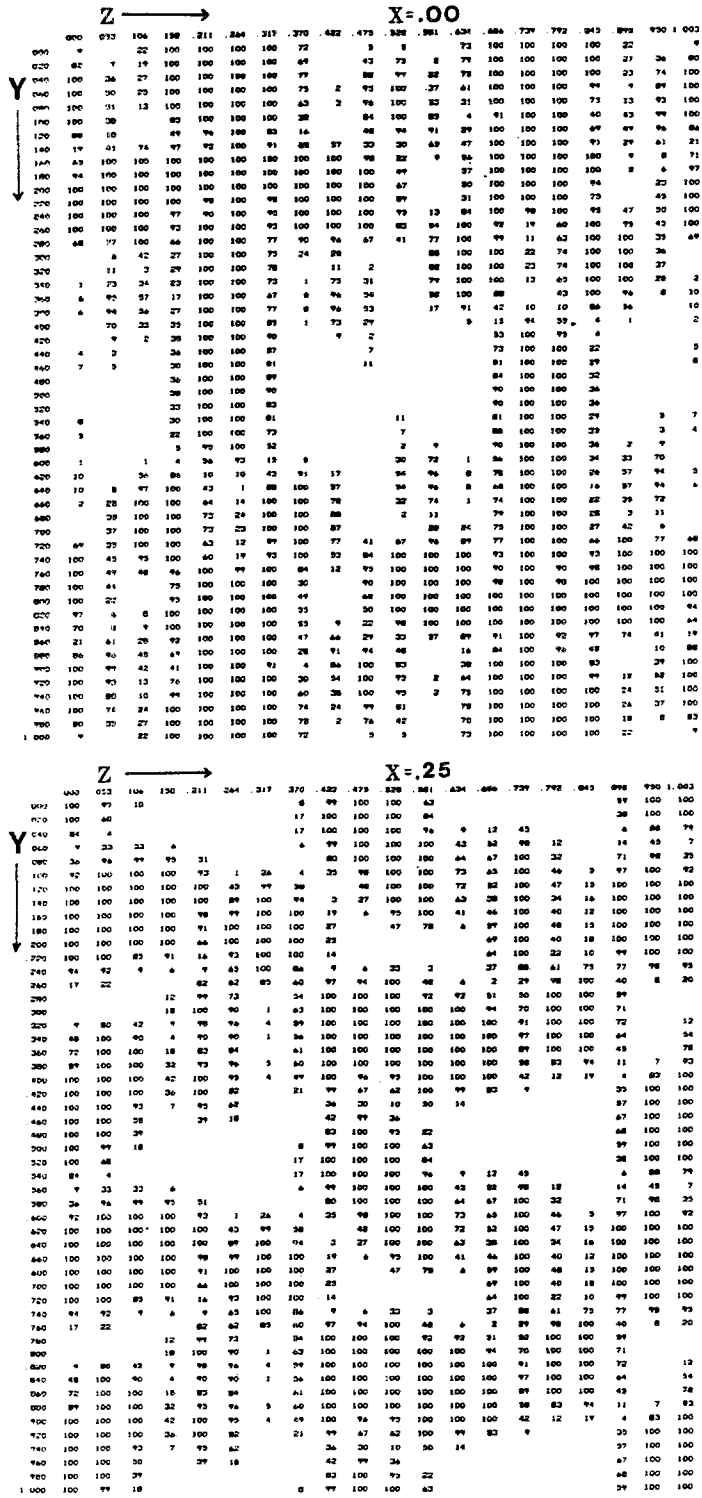

Fig. 5c. Packing diagrams of structure (**1**) with host and guest (hydrogens included) at $x = 0.0$ and $x = 0.25$.

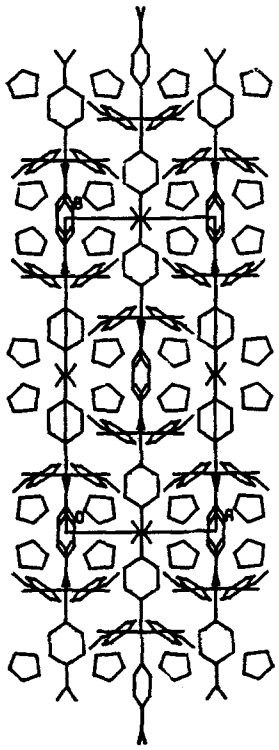

Fig. 6. Molecular packing in structure (**1**) viewed down the z-axis.

On the basis of previous work [3,7,22] these structures may be regarded as β-phases with a three-dimensional network of cavities interconnected by channels running parallel to the x and z axis (Figures 5a–c and 6). Figure 5a clearly shows (i) the disorder of the terminal vinyl carbon atoms about the diad, (ii) the propeller conformation of the 4-vinylpyridine ligands, (iii) the clearly defined geometry of the ligands (90°) resulting from the symmetry imposed diad and (iv) the isothiocyanate ligands running almost parallel to the a-axis.

The packing diagrams (OPEC [33], hydrogens included) of the host only are shown in Figure 5b and voids are clearly visible at $x = 0.0$, with the channels parallel to the x axis located around 0, 1/2, 0 and 0, 1/2, 1/2, inversion centres, b, and 0, 0, 0 and 0, 0, 1/2, inversion centres, a. Observation of Figure 5b at $x = 0.25$ shows the channels and interlinked cavities running parallel to the z axis. Observation of the packing diagram with host and guest (Figure 5c) at $x = 0.0$ shows the guest occupying the channels around 0, 0, 0 and 0, 0, 1/2, with the channels around the inversion centre, b, remaining empty. This results in four THF molecules in the unit cell (with their atoms at general positions) but related by a centre of symmetry. The host–guest packing diagram at $x = 0.25$ shows two new guests which sit in the cavities (linked by channels) in the vicinity of 1/4, 0.4,

TABLE VII. Torsion angles of the host in structures (**1**)–(**5**).

Torsion Angle	(**1**)	(**2**)	
N(1)–Ni(1)–N(41)–C(42)	37.6(9)°	36.1(9)°	
N(1)–Ni(1)–N(41)–C(46)	34.7(8)°	35.4(8)°	
N(1)–Ni(1)–N(21)–C(22)	42.5(8)°	43.0(8)°	
N(1)–Ni(1)–N(11)–C(12)	34.2(8)°	33.6(8)°	
	(**3**)	(**4**)	(**5**)
N(1)–Ni(1)–N(21)–C(22)	41.6(8)°	43.7(6)°	42.6(6)°
N(1)–Ni(1)–N(21)–C(26)	40.0(8)°	40.6(6)°	41.3(6)°
N(1)–Ni(1)–N(11)–C(12)	39.1(8)°	37.7(7)°	35.2(7)°
N(1)–Ni(1)–N(11)–C(16)	33.5(9)°	32.8(7)°	34.0(7)°

0.0 and 1/4, 0.54, 1/2. These two guests generate the remaining two guests by the inversion centres at 1/2, 1/2, 0 and 1/2, 1/2, 1/2. Thus all the guest atom positions are on general positions with four THF molecules being related by four inversion centres at Wyckoff special position a to generate the remaining four THF molecules. The remaining unoccupied voids about the inversion centres, Wyckoff special position b, are smaller than the occupied voids, but could accommodate the remaining cyclohexane (**1**) and cyclohexene (**2**). However a difference electron density map contoured in this region showed a very low electron density, less than 0.4 e/Å^3.

One of the factors that is considered to contribute to the enclathrating ability (and hence selectivity) of these hosts is the free rotation of the pyridine rings about their Ni–N bonds (free rotation of approximately 40° with H on the *ortho* position) allowing the host to adopt a suitable conformation and accommodate the guest [5]. The four torsion angles (Table VII) are slightly different from each other showing a nonregular propeller conformation of the host. The corresponding torsion angles in structures (**1**) and (**2**) do not differ significantly at the 3σ level [21], which may be expected as the difference in guest contents is very small.

One nonbonding contact [25] in structure (**2**) was found between the host, H(23) and the guest, C(3G) (2.82 Å < 3.05 Å, sum of van der Waals radii).

3.3. CLATHRATES (**3**), (**4**) AND (**5**)

In structures (**3**), (**4**) and (**5**) the nickel is at Wyckoff special position e at 1/2, 1/4, 0.55. Figure 4 shows the host with none of the ligands on the diad. Like structures (**1**) and (**2**) these structures crystallize in the same manner as the β-phase structures but with the cavities interconnected by channels running parallel to the x and y axis (Figures 7a,b).

Using structure (**4**) as an example, observation of the packing diagram (Figure 7b) of the unit cell section at $y = 0.0$ (host only) shows the channels parallel

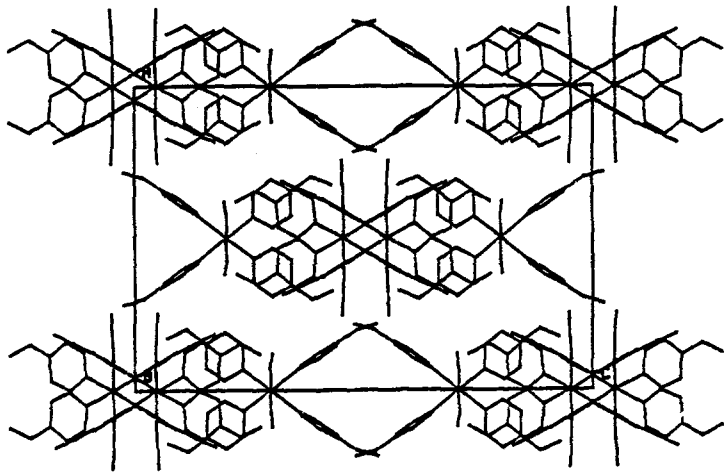

Fig. 7a. Molecular packing of the host in structure (4) viewed down the y-axis.

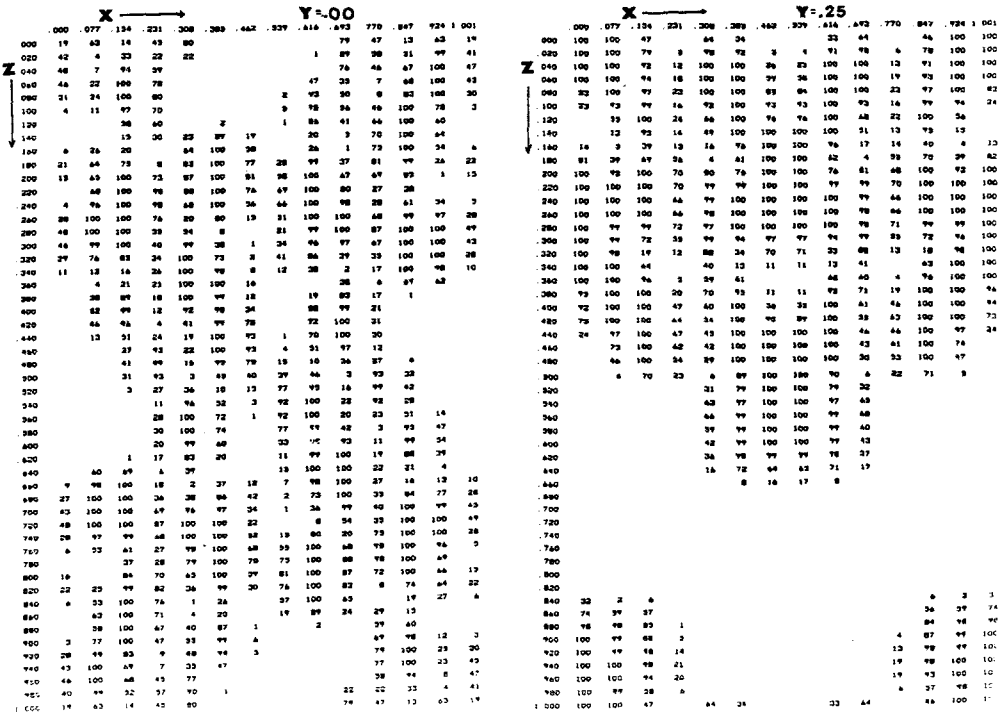

Fig. 7b. Packing diagrams of structure (4) with host only (hydrogens included) at $y = 0.0$ and $y = 0.25$.

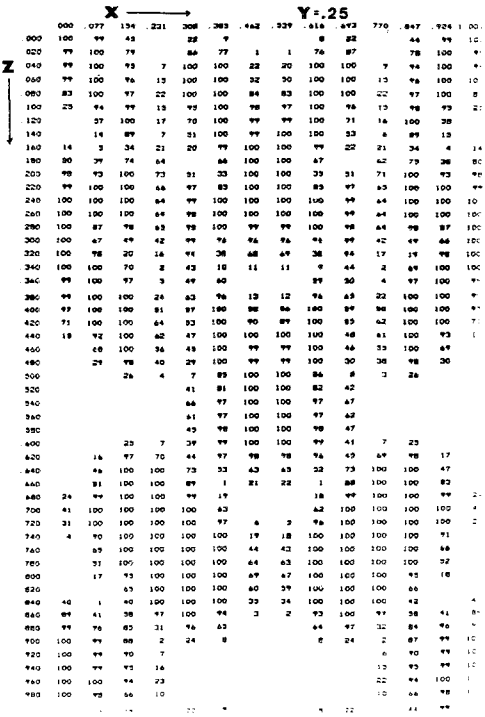

Fig. 7c. Packing diagrams of structure (**3**) with host and guest (hydrogens included) at $y = 0.25$.

to the y axis, located at the inversion centres, 0, 0, 1/2 and 1/2, 0, 0. At $y = 0.25$ Figure 7b shows the channel/cavity parallel to the x axis. This void is large and includes the inversion centre at 3/4, 1/4, 3/4 and the $\bar{4}$ sites at 0, 1/4, 5/8 and 1/2, 1/4, 7/8, Wyckoff special position *b*. (Note the small voids at 0, 1/4, 1/8 and 1/2, 1/4, 3/8 which are $\bar{4}$ sites, Wyckoff special position *a*.)

The packing diagram of structure (**3**) with the host and guest at $y = 0.25$ (Figure 7c) shows the packing of the guests in the channel with their atoms being disordered about and through the inversion centre and are connected by cavities with the $\bar{4}$ sites giving rise to large unoccupied voids ($\rho = 1.18$ g cm^{-3}, host : guest ratio 1 : 1).

The packing diagrams of structure (**4**) (Figure 7d) and structure (**5**) (Figure 7e) with the host and guest at $y = 0.25$ show the increased guest contents ($\rho = 1.25$ g cm^{-3}, host : guest ratio 1 : 1.4) filling the channels (inversion centres) and the cavities ($\bar{4}$ sites). In all three structures there is minimal host–guest interaction to the extent of small cavities between the host and guest, as is particularly noticeable in Figures 7d and 7e.

In these three structures the guest contents vary significantly. If the ability of the host's 4-vinylpyridine ligands in varying their conformation plays a role in its

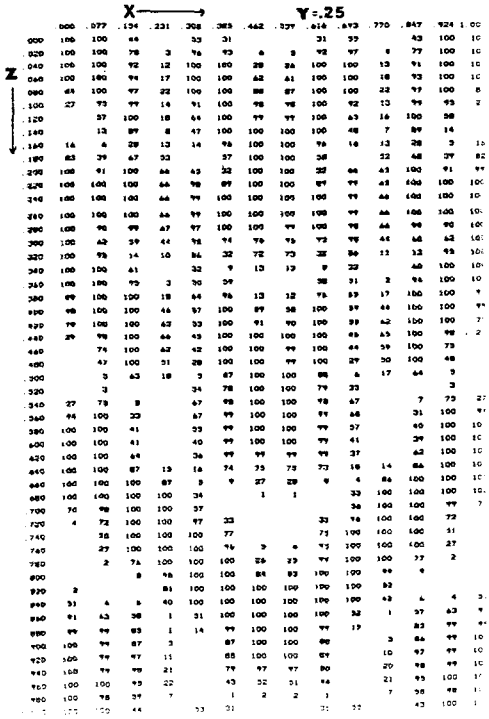

Fig. 7d. Packing diagrams of structure (**4**) with host and guest (hydrogens included) at $y = 0.25$.

enclathrating ability, this should be detected in comparing the torsion angles of structures (**3**), (**4**) and (**5**) (Table VII). In conjunction with the isomorphous nature of the host in these structures the torsion angles do not vary significantly, at the 3σ level [21], to account for the changing ratio of the two guests included nor the varying host : *total* guest ratio.

In each structure the guests are disordered owing to the mixture of two guest types and the symmetry of 1,3-cyclohexadiene not coinciding with the site symmetry. There is also very little host–guest interaction to minimize the guests' thermal motion (nonbonding contacts between host and guest were not found [25]).

3.4. CLATHRATE (**6**)

Structure (**6**) is the only structure in this study with the nickel at a general position, Wyckoff position *i*. Following the classification of previous work with the 4-ethylpyridine host [6], this structure is a γ-phase with the host atoms at general positions and the guest molecules (benzene only) located in cavities of centrosymmetric symmetry. Unlike the above structures in this study, the centrosymmetric benzene matches the symmetry of the cavities at the $\bar{1}$ sites. This structure also has guest molecules at general positions with all the guest molecules being well

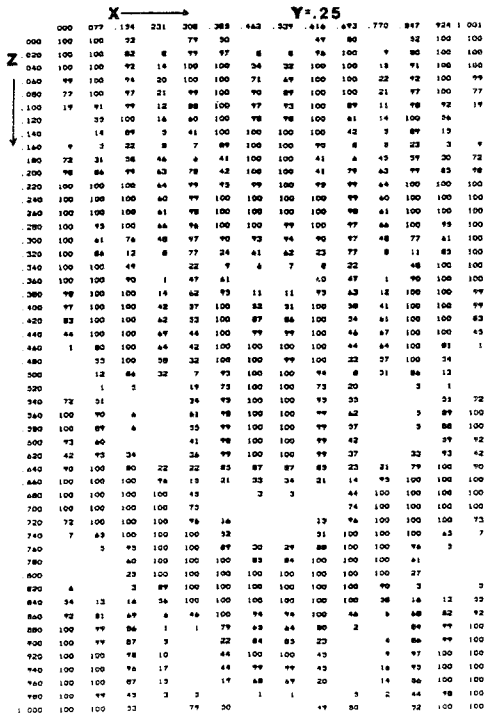

Fig. 7e. Packing diagrams of structure (**5**) with host and guest (hydrogens included) at $y = 0.25$.

ordered. The molecular diagrams show the channels down the x axis (Figure 8) and a channel parallel to the z axis (Figure 9). With a host : guest ratio of 1 : 3, these cavities are large and interlinked by channels, as shown by the packing diagrams in Figure 10a with host only. Figure 10b shows the packing efficiency of the host and guest, and at $y = 0.5$ the packing efficiency is shown to be poor as there are a number of voids remaining.

As with all previous structures the program PARST was used to detect any intermolecular contact less than the sum of their van der Waals radii, of which none were found [25]. Of all the structures, the observed lack of interaction between the host and guest in structure (**6**) is most surprising as none of the guest atoms are disordered and their temperature factors are low, varying from 0.08–0.19 Å^2. With no evidence of host–guest interaction in the crystal structure we are unable to account for the large host : guest ratio.

3.5. PACKING VOLUMES

The packing density (packing volume) of each clathrate was analysed in an attempt to explain the observed host to guest and guest1/guest2 ratios. The packing density of structures (**1**)–(**6**) and the α-phase [7] (host only) are listed in Table VIII,

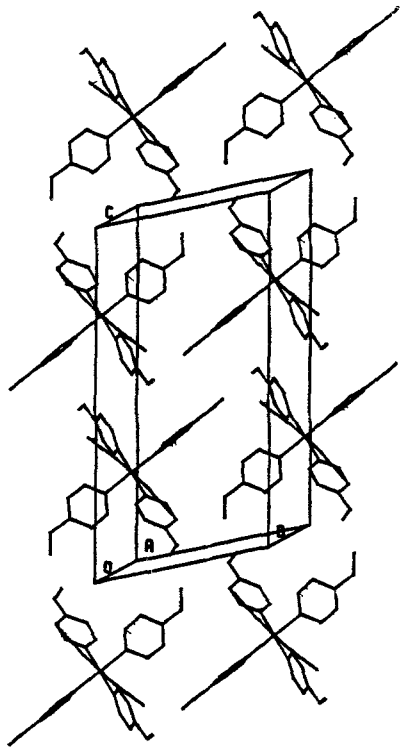

Fig. 8. Molecular packing of the host in structure (**6**) viewed down the x-axis.

TABLE VIII. Packing densities and volume comparisons.

Structure	Packing density Vol/non-hydrogen atom Å^3	Volume/guest molecule Å^3	Volume[a] 'per guest' Å^3	% Packing efficiency per void per guest	Total volume of guest per host Å^3
α-phase	19.9	–	–	–	–
(**1**)	20.8	123.7	81.1	66	162.2
(**2**)	20.8	124.9	80.7	65	161.4
(**3**)	21.2	170.1	86.0	51	86.0
(**4**)	19.9	116.0	89.2	77	124.9
(**5**)	19.9	114.8	85.8	75	120.1
(**6**)	20.7	135.3	88.2[b]	65	264.6
(**7**)	20.8	121.4	78.4[b]	65	156.8

[a] Obtained from theoretical volumes of guest molecules.

[b] Only one guest type and is therefore the theoretical volume.

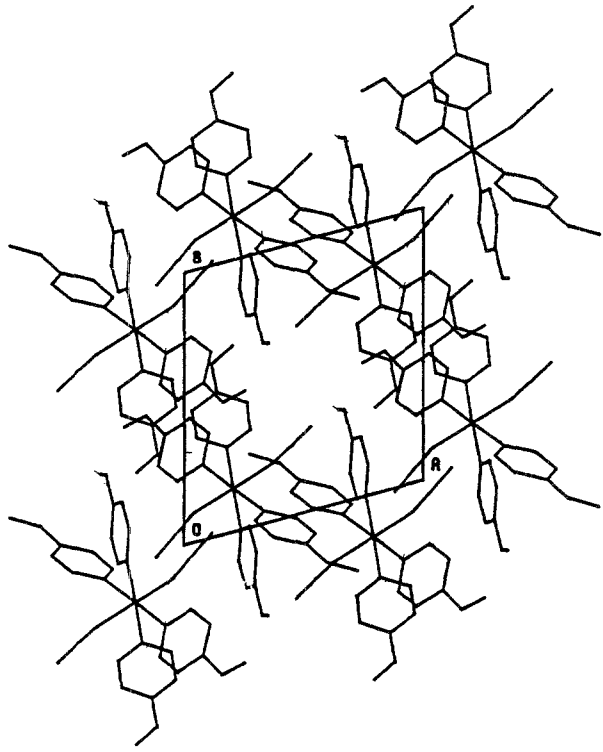

Fig. 9. Molecular packing of the host in structure (**6**) viewed down the z-axis.

column 1 and were obtained by the usual expression 'volume of unit cell/number of non-hydrogen atoms in the unit cell'. High packing volumes may indicate disorder of the vinyl group of the host (as in structures (**1**) and (**2**)) and/or disorder of the guest (as in structures (**1**)–(**5**)) and/or the presence of large unoccupied voids (as in structure (**3**)) and/or a high percentage of guest contents (as in structure (**6**)).

Structure (**3**) has the highest packing volume of 21.2 Å^3 with the $\bar{4}$ sites unoccupied. Structures (**1**) and (**2**) have the second highest packing volume of 20.8 Å^3. Structure (**6**) with ordered host and guest atoms, but with the higher host : guest ratio of 1 : 3, has a packing volume of 20.7 Å^3 which can only be accounted for by poor packing between the host and guest molecules. Structures (**4**) and (**5**) with both the $\bar{1}$ and $\bar{4}$ sites occupied by guest molecules have the lowest packing volume of 19.9 Å^3 which is equal to that of the α-phase.

Another way of comparing packing efficiencies is the comparison of the volume available to the guests and the efficiency with which the guest fills this volume. The volume occupied by host molecules was obtained by dividing the unit cell volume of the α-phase by the number of host molecules [7]. To calculate the total volume available to guest molecules in structures (**1**)–(**6**), the total volume occu-

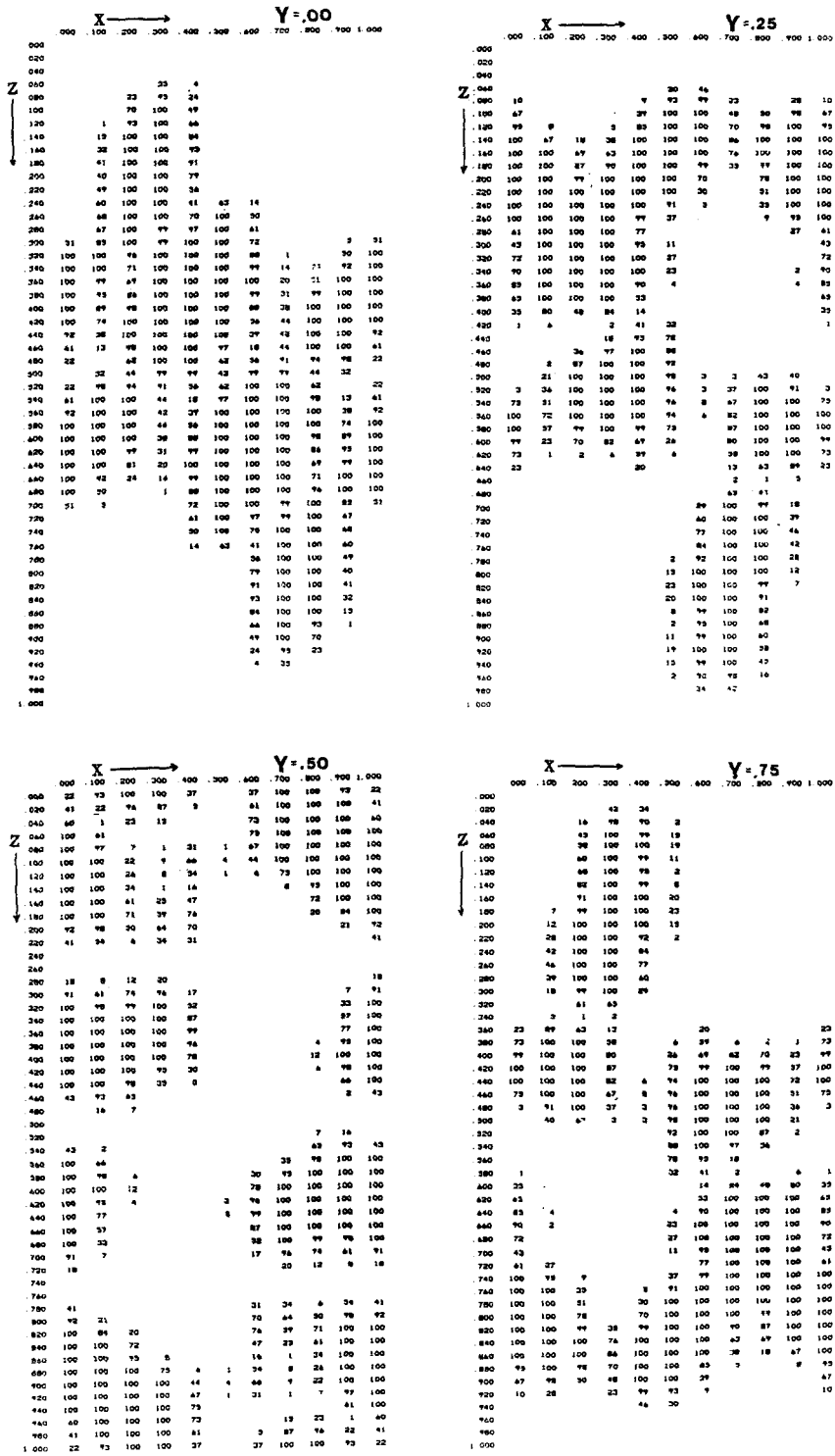

Fig. 10a. Packing diagrams of structure (**6**) with host only (hydrogens included) at $y = 0.0$, $y = 0.25$, $y = 0.5$, $y = 0.75$.

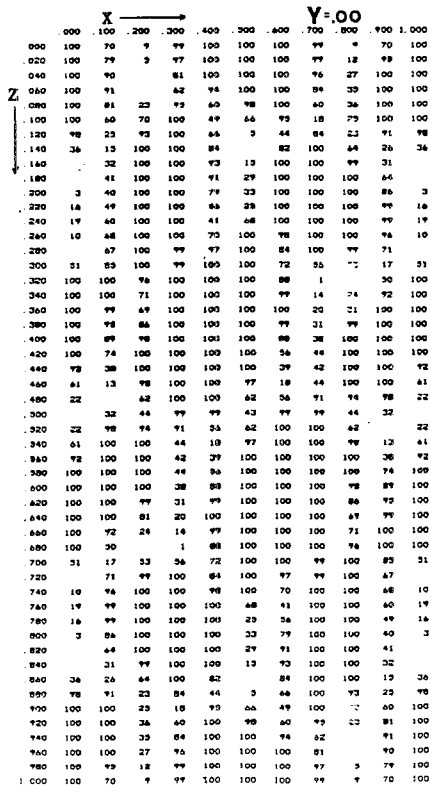

Fig. 10b. Packing diagrams of structure (**6**) with host and guest (hydrogens included) at $y = 0.0$ and $y = 0.5$.

pied by host was subtracted from the respective unit cell volume of the clathrates. This total available volume divided by the number of guest molecules per unit cell gives the volume available per guest molecule. These values expressed as volume/guest molecule (Å^3) are listed in Table VIII with structure (**1**) as an example: volume/guest molecule = $[(\mathrm{Vol}_{\text{unit cell}})-(774.4 \times 4)] \div 8 = 123.7$ Å^3.

The theoretical volume for each guest type was calculated using the volumes of appropriate fragments as determined by Kitaigorodsky [32]. Taking the molecular ratios of the guests into account for structures (**1**)–(**5**) the theoretical volumes 'per guest' were calculated. These values are listed in Table VIII with structure (**1**) as an example: volume of THF = 78.4 Å^3, volume of cyclohexane = 102.6 Å^3. Volume 'per guest' = $(78.4 \times 0.89) + (102.6 \times 0.11) = 81.1$ Å^3.

We now introduce a new parameter for analysing clathrate structures: packing efficiency per void per guest. The most efficient packing of the guests in the 'available volumes' is unity. Again structure (**1**) serves as an example: packing efficiency per void per guest = volume 'per guest'/'available volume' = 81.1 Å^3/123.7 Å^3 = 0.66 or, percentage packing efficiency per void per guest = 66%. The percentage

packing efficiency per void per guest values follow the same trend (but inversely) as the packing volume values with structures (**4**) and (**5**) having the highest percentage packing efficiency per void per guest values of 77 and 75%, respectively, and structure (**3**) having the lowest, 51%. As the same trend was obtained this shows that the overall packing volume (overall packing efficiency) of these clathrate structures is dominated by the packing efficiency per void per guest.

The packing values obtained may not be taken as absolute values as the total volume unoccupied by host does not necessarily imply that it is available for guest occupation. It is interesting to note that the volume of each guest ratio pair (or volume 'per guest') is fairly constant for structures (**1**)–(**5**) but does not account for the changing ratios of guests included nor the total host to guest ratios.

4. Conclusion

This study has shown a systematic variation of the type of guest and the quantity of guest enclathrated by the host $[Ni(NCS)_2(4\text{-ViPy})_4]$. As previous studies had shown that THF is not included as guest (see Section 2.2) our intention was to obtain clathrates with only cyclohexane, cyclohexene, 1,3-cyclohexadiene, 1,4-cyclohexadiene and benzene as guest molecules. Although the inclusion of THF compounded our results, we have shown that the question as to whether a molecule may or may not be included depends on the presence of other molecules. In effect, we have studied the competition of different chemical species for cocrystallization with the host. In this regard the trend is observed that increasing the number of π electrons (with volume and shape essentially constant) in the guest molecule, increases its potential for enclathration by the host.

This paper indicates the possible complexity that may arise when crystals are obtained from a solution of more than one solvent. Inclusion compounds are often obtained with the potential host dissolved in one solvent and added to a second solvent, with the intention of obtaining an inclusion compound with the second solvent as guest. As these structures may contain disordered guests and the crystal density determination may be compounded by the relative ease of loss of guest, it is noted that an additional method must be used to confirm the crystal contents. In this work we used NMR spectroscopy although microanalysis and mass spectrometry are often used.

It has been considered (e.g. Reference [5]) and is still currently accepted (e.g. Reference [36]), that the most significant structural feature that enables Werner complexes to accommodate a variety of guest molecules is the ability of the substituted pyridines to rotate about their Ni–N bonds. *This work, and previous studies, show that the conformational freedom of the substituted pyridines is not the primary reason for the clathrating ability of Werner clathrates.*

The complex $[Ni(NCS)_2(4\text{-methylpyridine})_4]$ has been shown to form inclusion compounds with many guests; however, the complex $[Ni(NCS)_2$ (3,5-dimethylpyridine)$_4]$ does not form inclusion compounds. Conformational energy

studies [13] of these two hosts have shown their respective conformations to be almost identical and that the conformational energy of these complexes is almost exclusively governed by the *ortho*-hydrogens on each base. "The extent of rotation allowed by the 3,5-dimethylpyridines is, therefore, not the factor which governs clathrate formation" (quoted from Reference [13]).

Structures (**3**), (**4**) and (**5**) are isomorphous with respect to the host, yet they have a significant difference in the total amount of guest and the type of guest enclathrated. This clearly shows that the ability of the 4-vinylpyridine ligands to rotate about their Ni–N bonds does not play a significant role in the selection of different guests.

When the $Ni–N_{cs}–C_s$ bond angle differs from 180°, the conformation of the NCS group around the Ni–N coordination bond plays an important role in determining the overall molecular shape of the host complex. Its relevance to clathrate formation is confirmed, as all six clathrate structures have the isothiocyanate ligands *trans*. The only observation of the *cis* conformation was in the α-phase [7].

This study indicates that the process of cocrystallization of the host and guest must occur simultaneously as a very small difference in the guest molecule results in a significant change in the crystal structure. For example, structures (**2**) (P_{bcn}) and (**3**) ($I4_1/a$) differ significantly, yet these differences were induced by the subtle differences of cyclohexene and 1,3-cyclohexadiene, respectively. This shows the effect that the guest molecules have on the host packing and the interplay that the host and guest have on each other during cocrystallization.

Charge-transfer interactions between the host and guest are not confirmed and shortening of intermolecular distances with respect to the sum of the van der Waals radii between the host and guest is not observed. No correlation is observed between host conformation and guest contents. *We conclude that this host's selectivity by enclathration cannot be accounted for by solid state structural analysis.*

In an attempt to account for the selective guest ratios observed in this work, we have extended our analysis of these clathrates in obtaining their thermodynamic parameters by thermogravimetric analysis and solubility studies, and it has been shown that the observed guest ratios are related to solubility [31].

Acknowledgements

We thank Dr. Margaret Niven for data collection and helpful discussion and the Council of Scientific and Industrial Research (CSIR) for financial support. Laurence Lavelle would like to thank the CSIR for their support in the form of non-contract Graduate Scholarships and The University of Cape Town for a Graduate Fellowship and for the Sir Robert Kotze and Harry Crossley Bursaries.

References

1. Part 12, L.R. Nassimbeni, M.L. Niven, and M.W. Taylor: *Acta Crystallogr.* **B46**, 354 (1990).
2. W.D. Schaeffer, W.S. Dorsey, D.A. Skinner, and J. Christian: *J. Am. Chem. Soc.* **79**, 5870 (1957).

3. W. Kemula, D. Sybliska, and J. Lipkowski: *J. Chromatogr.* **218**, 465 (1981).
4. J. Lipkowski, P. Starzewski, and W. Zielenkiewicz: *Pol. J. Chem.* **56**, 349 (1982).
5. J. Lipkowski, in *Inclusion Compounds*, eds. J.L. Atwood, J.E.D. Davies, and D.D. MacNicol, Academic Press, New York, Vol. 1, Ch 3. pp. 59–103 (1984).
6. M.H. Moore, L.R. Nassimbeni, and M.L. Niven: *J. Chem. Soc. Dalton Trans.* 2125 (1987); *J. Chem. Soc. Dalton Trans.* 369 (1990).
7. M.H. Moore, L.R. Nassimbeni, M.L. Niven, and M.W. Taylor: *Inorg. Chim. Acta.* **115**, 211 (1986).
8. M.H. Moore, L.R. Nassimbeni, and M.L. Niven: *Inorg. Chim. Acta.* **131**, 45 (1987).
9. L.R. Nassimbeni, M.L. Niven, and A.P. Suckling: *Inorg. Chim. Acta* **159**, 209 (1989).
10. L. Lavelle, L.R. Nassimbeni, M.L. Niven, and M.W. Taylor: *Acta Crystallogr.* **C45**, 591 (1989).
11. L.R. Nassimbeni, M.L. Niven, and M.W. Taylor: *J. Chem. Soc. Dalton Trans.* 119 (1989).
12. L.R. Nassimbeni, M.L. Niven, and M.W. Taylor: *Inorg. Chim. Acta* **132**, 67 (1987).
13. L.R. Nassimbeni, S. Papanicolaou, and M.H. Moore: *J. Incl. Phenom.* **4**, 31 (1986).
14. C. Orvig: *J. Chem. Educ.* **62**, 82 (1985).
15. A.C.T. North, D.C. Phillips, and F.S. Mathews: *Acta Crystallogr.* **A24**, 351 (1968).
16. G.M. Sheldrick: 'The SHELX-76 program system', in *Computing in Crystallography*, eds. H. Schenk, R. Olthof-Hazekamp, H. van Koningsveld, and G.C. Bassi, Delft University Press, p. 34 (1978).
17. W.J.A.M. Peterse and J.H. Palm: *Acta Crystallogr.* **20**, 147 (1966).
18. L. Pauling: *The Nature of the Chemical Bond*, Cornell University Press, Ithaca, New York, 3rd edn. (1960).
19. D.T. Cromer and J.B. Mann: *Acta Crystallogr.* **A24**, 321 (1968).
20. R.F. Stewart, E.R. Davidson, and W.T. Simpson: *J. Chem. Phys.* **42**, 3175 (1965).
21. W. Klyne and V. Prelog: *Experienta* **16**, 521 (1960).
22. J. Lipkowski, K. Suwinska, G.D. Andreetti, and K. Stadnicka: *J. Mol. Struct.* **75**, 101 (1981).
23. D.R. Bond, G.E. Jackson and L.R. Nassimbeni: *S. Afr. J. Chem.* **36**, 19 (1983).
24. W.D.S. Motherwell: 'The PLUTO program for plotting molecular and crystal structures', Cambridge University, England, unpublished.
25. M. Nardelli: *Comput. Chem.* **7**, 95 (1983).
26. ALCHEMY, Tripos Associates Inc., 6548 Clayton Road, St. Louis, Missouri, 63117.
27. P. Main, S.E. Hull, L. Lessinger, G. Germain, J.P. Declerq, and M.W. Woolfson: MULTAN 78, University of York, England and University of Louvain, Belgium (1978).
28. Laurence Lavelle: Honours Thesis, Department of Chemistry, University of Cape Town, Rondebosch 7700, South Africa (1986).
29. Laurence Lavelle: Master Thesis, Department of Chemistry, University of Cape Town, Rondebosch 7700, South Africa (1988).
30. *The Aldrich Library of NMR Spectra*, 2nd ed. (1983).
31. L. Lavelle: *J. Chem. Soc. Dalton Trans.* 3511 (1992).
32. A.I. Kitaigorodsky: *Molecular Crystals and Molecules*, Academic Press, New York (1973).
33. A. Gavezzotti: OPEC, *J. Am. Chem. Soc.* **105**, 5220 (1983).
34. J. Votinský, J. Kalousová, and L. Beneš: *J. Incl. Phenom.* **14**, 19 (1992).
35. L. Pang, E.A.C. Lucken, and G. Bernardinelli: *J. Incl. Phenom.* **13**, 63 (1992).